doi:10.1093/brain/awy033 BRAIN 2018: 141; 1094–1110 | 1094

BRAIN
A JOURNAL OF NEUROLOGY

Chondroitin sulfate proteoglycans as novel drivers of leucocyte infiltration in multiple sclerosis

Erin L. Stephenson,[1] Manoj K. Mishra,[1] Daniel Moussienko,[1] Nataly Laflamme,[2] Serge Rivest,[2] Chang-Chun Ling[3] and V. Wee Yong[1]

Multiple sclerosis presents with profound changes in the network of molecules involved in maintaining central nervous system architecture, the extracellular matrix. The extracellular matrix components, particularly the chondroitin sulfate proteoglycans, have functions beyond structural support including their potential interaction with, and regulation of, inflammatory molecules. To investigate the roles of chondroitin sulfate proteoglycans in multiple sclerosis, we used the experimental autoimmune encephalomyelitis model in a time course study. We found that the 4-sulfated glycosaminoglycan side chains of chondroitin sulfate proteoglycans, and the core protein of a particular family member, versican V1, were upregulated in the spinal cord of mice at peak clinical severity, correspondent with areas of inflammation. Versican V1 expression in the spinal cord rose progressively over the course of experimental autoimmune encephalomyelitis. A particular structure in the spinal cord and cerebellum that presented with intense upregulation of chondroitin sulfate proteoglycans is the leucocyte-containing perivascular cuff, an important portal of entry of immune cells into the central nervous system parenchyma. In these inflammatory perivascular cuffs, versican V1 and the glycosaminoglycan side chains of chondroitin sulfate proteoglycans were observed by immunohistochemistry within and in proximity to lymphocytes and macrophages as they migrated across the basement membrane into the central nervous system. Expression of versican V1 transcript was also documented in infiltrating CD45+ leucocytes and F4/80+ macrophages by *in situ* hybridization. To test the hypothesis that the chondroitin sulfate proteoglycans regulate leucocyte mobility, we used macrophages in tissue culture studies. Chondroitin sulfate proteoglycans significantly upregulated pro-inflammatory cytokines and chemokines in macrophages. Strikingly, and more potently than the toll-like receptor-4 ligand lipopolysaccharide, chondroitin sulfate proteoglycans increased the levels of several members of the matrix metalloproteinase family, which are implicated in the capacity of leucocytes to cross barriers. In support, the migratory capacity of macrophages *in vitro* in a Boyden chamber transwell assay was enhanced by chondroitin sulfate proteoglycans. Finally, using brain specimens from four subjects with multiple sclerosis with active lesions, we found chondroitin sulfate proteoglycans to be associated with leucocytes in inflammatory perivascular cuffs in all four patients. We conclude that the accumulation of chondroitin sulfate proteoglycans in the perivascular cuff in multiple sclerosis and experimental autoimmune encephalomyelitis boosts the activity and migration of leucocytes across the glia limitans into the central nervous system parenchyma. Thus, chondroitin sulfate proteoglycans represent a new class of molecules to overcome in order to reduce the inflammatory cascades and clinical severity of multiple sclerosis.

1 Hotchkiss Brain Institute and the Department of Clinical Neurosciences, University of Calgary, Alberta, Canada
2 Department of Molecular Medicine, CHU de Quebec Research Center, Laval University, Quebec, Canada
3 Department of Chemistry, University of Calgary, Alberta, Canada

Correspondence to: Prof. V. Wee Yong, PhD
University of Calgary
3330 Hospital Drive
Calgary, Alberta T2N4N1
Canada
E-mail: vyong@ucalgary.ca

Received June 19, 2017. Revised December 27, 2017. Accepted January 4, 2018. Advance Access publication March 1, 2018

Keywords: multiple sclerosis; chondroitin sulfate proteoglycans; versican; perivascular cuff; neuroinflammation

Abbreviations: CSA = chondroitin sulfate A; CSPG = chondroitin sulfate proteoglycan; EAE = experimental autoimmune encephalomyelitis; LPS = lipopolysaccharide; MMP = matrix metalloproteinase

Introduction

Multiple sclerosis is a chronic demyelinating disease of the CNS that presents with both immune abnormalities and neurodegenerative changes. A hallmark is the extravasation of activated lymphocytes into the CNS parenchyma, accompanied by myelin breakdown and axonal loss (Noseworthy *et al.*, 2000; Frohman *et al.*, 2006; Trapp and Nave, 2008). Routes of entry of immune cells into the CNS include subpial meningeal infiltration, passage across the fenestrated ependymal layer of the choroid plexus, and transmigration through the basement membranes of post-capillary venules (Sorokin, 2010; Ransohoff and Engelhardt, 2012). Leucocyte transmigration across post-capillary venules involves a multi-step cascade (Engelhardt and Ransohoff, 2005) where circulating leucocytes are initially slowed by interaction between selectin receptors and their mucin ligands. For example, lymphocytes expressing PSGL-1 are slowed by interaction with P-selectin-expressing endothelial cells (Kerfoot and Kubes, 2002). CD44 and α4 integrins can act to slow leucocytes in place of selectins (Brocke *et al.*, 1999). Slowed leucocytes can sense chemokines or other chemoattractant molecules presented at the endothelial surface; the chemokine signalling activates the adhesive integrins that then mediate firm adhesion of leucocytes to the endothelium. This is followed by lymphocyte diapedesis across the endothelial cell barrier through paracellular or transcellular routes.

A post-endothelial step in leucocyte migration into the brain parenchyma from post-capillary venules is their crossing of two basement membranes; first the endothelial basement membrane, and secondly the parenchymal basement membrane/glial limitans (Tran *et al.*, 1998; Archambault *et al.*, 2005; Agrawal *et al.*, 2006; Engelhardt, 2006; Toft-Hansen *et al.*, 2006; Owens *et al.*, 2008). Before leucocytes migrate across the second parenchymal basement membrane/glial limitans they accumulate in the perivascular space, forming a visible perivascular cuff. The accumulation of immune cells in the perivascular space may act as a regulatory checkpoint, requiring additional enhancing stimuli for leucocytes to cross the parenchymal basement membrane and invade the CNS. Fundamental gaps in knowledge still remain, including the signals to stimulate leucocytes to transmigrate across the parenchymal basement barrier to inflict neural injury.

Previous studies have illustrated how extracellular matrix components can orchestrate leucocyte activation and infiltration into the CNS and have direct consequences on inflammatory outcomes. For example, laminin-511 (α5, β1 and γ1) inhibits T lymphocyte migration by interfering with interactions between α6β1 integrin and laminin-411 (α4, β1 and γ1 chains) (Wu *et al.*, 2009). Heparan sulfate proteoglycans interact with selectin ligands on immune cells, as well as by binding chemokines and enhancing their function (Parish, 2006). Hyaluronan accumulates in regions of immune cell infiltration in an inflammatory model of multiple sclerosis, experimental autoimmune encephalomyelitis (EAE), and enhances the pro-inflammatory nature and trafficking of T lymphocytes (Kuipers *et al.*, 2016).

The chondroitin sulfate proteoglycans (CSPGs) are components of the extracellular matrix and they are elevated at the expanding edge of multiple sclerosis lesions (Sobel and Ahmed, 2001). Besides being inhibitors of axonal regeneration (Galtrey and Fawcett, 2007), and of remyelination (Lau *et al.*, 2012; Keough *et al.*, 2016), CSPGs have pro-inflammatory characteristics in peripheral tissues that include the ability to enhance leucocyte migration, activate leucocytes, and bind chemokines/cytokines (Haylock-Jacobs *et al.*, 2011). There are four lectin-binding CSPGs (lecticans) in the CNS: brevican, neurocan, aggrecan, and versican. Versican, itself comprises four isoforms (V0, V1, V2 and V3; encoded by the *VCAN* gene). In the normal adult CNS, aggrecan is expressed exclusively around perineuronal nets (Matthews *et al.*, 2002; Galtrey *et al.*, 2008; Morawski *et al.*, 2012), but the other lecticans are also present in perineuronal nets (Carulli *et al.*, 2006). Versican V2 is also found in myelinated tracts at nodes of Ranvier (Dours-Zimmermann *et al.*, 2009). Versican V1 is normally expressed at low levels in the adult CNS but is elevated in areas of CNS trauma such as lysolecithin-induced demyelination (Keough *et al.*, 2016). Macrophages, particularly the pro-inflammatory subtype, are known to express versican V1 (Toeda *et al.*, 2005).

In this study, we sought to determine whether CSPGs are altered in EAE and in multiple sclerosis, focusing on the perivascular cuff as an entry point of leucocytes into the CNS. We examined the functions of the altered lectican CSPGs, particularly on their pro-migratory roles for macrophages. The culmination of these experiments contributes to the new direction in considering CSPGs as novel drivers of leucocyte infiltration and neuroinflammation in multiple sclerosis.

Materials and methods

Animals and experimental autoimmune encephalomyelitis

All procedures were carried out in accordance with guidelines of the Canadian Council of Animal Care and have received approval by local ethics committee. EAE was induced

according to previously described protocols in this laboratory (Giuliani *et al.*, 2005). Eight- to 10-week-old female C57Bl/6 mice were used as there is a female bias in multiple sclerosis. Induction was by immunization with myelin oligodendrocyte glycoprotein (MOG_{35-55}, peptide 35–55, synthesized by the Peptide Facility of the University of Calgary), emulsified in complete Freund's adjuvant (CFA) containing 10 mg/ml of heat inactivated *Mycobacterium tuberculosis* H37RA (Difco). Fifty microlitres (200 µg) of MOG_{35-55} was injected subcutaneously into each hind flank. At time of MOG_{35-55} immunization and again 2 days later, each animal received 300 ng of pertussis toxin intraperitoneally. Mice were evaluated daily for weight loss, and scored daily for clinical signs of EAE with a 15-point scale (Weaver *et al.*, 2005). Thus, at Days 7 (preclinical), 12 (expected onset of clinical signs), 18 (expected peak clinical severity), and 32 (post-peak), thoracic spinal cord and cerebellum were collected for immunohistochemistry, while lumbar cords were used for PCR and western blots. These regions were selected because pathology in EAE develops first in the caudal spinal cord, and then ascends rostrally; moreover, the cerebellum is a brain region with prominent inflammatory perivascular cuffs in EAE-afflicted animals (Agrawal *et al.*, 2013).

Multiple sclerosis brain specimens

Post-mortem frozen archived brain tissue from four cases of multiple sclerosis obtained from UK Multiple Sclerosis Tissue Bank (Imperial College, London, courtesy of Dr Richard Reynolds) were used. These four cases were selected from our frozen archives based on our previous finding that they contained active lesions (Agrawal *et al.*, 2013). All multiple sclerosis tissues were obtained and used with ethics approval. Brain samples were from three females and one male, aged 39 to 84 years old, with multiple sclerosis durations between 21 to 45 years. One sample did not have a specified multiple sclerosis type, one case was secondary progressive and the remaining two were diagnosed as relapsing-remitting multiple sclerosis. Post-mortem time ranged from 8 h to a maximum of 18 h. One frozen unfixed tissue block (~4 cm^2 surface area) for each case was cut into three or four blocks, and each block was sectioned into 10-µm thin sections using a cryostat before staining. Sections were fixed immediately prior to staining with antibodies noted in Supplementary Table 1.

Histology

To study the progression of EAE, EAE mice were sacrificed at various time points post-immunization representing pre-onset (Day 7), onset (Day 12), peak (Day 18), and chronic (Day 32) stages. Mice were given a lethal dose of anaesthetic (ketamine/xylazine), followed by transcardial perfusion of 20 ml ice-cold phosphate-buffered saline (PBS) solution injected into the left ventricle. Spinal cords were dissected and flash-frozen in O.C.T. compound and stored at −80°C. Each block was sectioned into 20-µm thick sections using a cryostat, mounted on glass slides and stored at −20°C.

Haematoxylin eosin/Luxol fast blue

We have previously described a semi-quantitative method to analyse the level of inflammation in the spinal cord of EAE mice (Goncalves DaSilva and Yong, 2009). EAE spinal cords were stained with haematoxylin/eosin and Luxol fast blue to determine tissue and myelin integrity, respectively. The number and location (i.e. parenchymal lesion showing more advanced disease activity versus inflammation confined to the subpial regions) of inflammatory lesions in separate sections in EAE were recorded to create a general histological inflammation score. We used histological inflammation to corroborate EAE clinical score. The advantage of this method is that it gives a measure of the burden of inflammation in the spinal cord, and is not skewed by lesions that have an over-representative effect on physical disability due to their neuroanatomical location.

Immunohistochemistry

Slides were removed from −20°C storage, thawed to room temperature and hydrated with PBS. Before staining tissues were post-fixed with −20°C methanol for 10 min and rinsed with PBS. Primary antibodies to the core protein of CSPG members required chondroitinase ABC digestion (0.2 U/ml in PBS) for 30 min at 37°C to remove the glycosaminoglycans that would otherwise impede detection. Slides were then washed with PBS and blocked for 1 h with a 10% horse serum containing 1% bovine serum albumin and 0.1% cold fish-skin gelatin buffer. Primary antibodies (Supplementary Table 1) were applied to tissue sections and left overnight at 4°C. All subsequent washes were with PBS-0.0125% Triton™ X-100. Species-specific secondary antibodies were conjugated to Alexa Fluor® 488 or Alexa Fluor® 594 and incubated along with nuclear yellow (1:1000) for 1 h following a rinse. Slides were mounted with gelvatol. Sections were examined using Olympus Fluoview FV10i confocal microscope.

Because of the high level of background staining in the vasculature, contributed to by non-specific IgG binding, all immunohistochemical stains were accompanied by secondary antibody controls. Chondroitin sulfate A (CSA) and CS56 primary antibodies are mouse IgMs, and thus are at a greater risk of non-specific staining. To ensure true staining, all primary/secondary stains were compared against a non-specific mouse IgM stained with a secondary antibody. The presence of the Triton™ X-100 in the PBS washes also reduced non-specific staining. While the CSA antibody was a mouse antibody used in mice to detect CSPGs, the CSA antibody also produced similar findings in human multiple sclerosis tissue as described below.

The antibody to versican V1 recognizes the glycosaminoglycan beta domain, and the versican V2 antibody recognizes the glycosaminoglycan alpha domain, both of which are present in the versican V0 splice isoform. However, due to the lack of co-localization of versican V1/V0 and versican V2/V0 in similar regions, we attributed the staining of versican V1 to primarily the V1 isoform, and the V2/V0 staining to V2.

Imaris quantification

The Imaris software (Bitplane, Switzerland) was used to determine the percentage of DAPI+ cells within the perivascular cuff in EAE that were Iba1+ or CD3+. CD3 and Iba1-labelled areas of a cell were rendered as surfaces, and the nuclear DAPI was rendered as spots. The Xtension program in Imaris 'surface close to spots' was used to calculate the nuclei that were within 2 µm of CD3+ or Iba1+ staining to give the

best approximation of the number of CD3+ and Iba1+ cells within cuffs.

Imaris was also used to quantify the number and distance of CD45+ cells outside of cuffs. Here, pan-laminin-detected cuffs were rendered as a surface and CD45+ cells were rendered as spots. 'Distance transformation', an Xtension component in Imaris, calculated the distance of every spot (i.e. CD45+ cell) from the cuff surface. A cut-off distance of 100 µm from the perivascular cuff was chosen based on our initial observation that most perivascular cuffs were greater than 200 µm apart from one another.

In a previous study (Keough *et al.*, 2016), we reported that a CSPG-lowering compound, peracetylated-4-F-*N*-acetylglucosamine (fluorosamine), alleviated EAE clinical severity when drug was initiated (50 mg/kg intraperitoneally) from Day 15 (a time point when mice were at peak clinical signs) daily until Day 26 when mice were killed. The spinal cord specimens collected from that study were used for the Imaris quantitation in the current study to examine the extent of leucocyte transmigration across perivascular cuffs into the CNS parenchyma.

Versican cRNA probe and *in situ* hybridization

Coronal sections were mounted on glass slides and *in situ* hybridization histochemical localization of versican V1 (*Vcan*) mRNA was performed using ^{35}S-labelled cRNA probes. A 1382-bp fragment (6016–7397 bases) specific to versican V1 cDNA was cloned from a mouse brain RNA library. The TOPO blunt constructed plasmid was linearized with HindII to generate antisense probe, T7 RNA polymerase was then used to produce radioactive cRNA antisense copies. Riboprobe synthesis and preparation and *in situ* hybridization were performed according to a protocol described previously (Laflamme *et al.*, 2001). Dual labelling combining immunocytochemistry and *in situ* hybridization was performed as described previously (Laflamme *et al.*, 2001) to localize versican V1 transcripts in CD45+ leucocytes or F4/80+ microglia/macrophages.

Real-time polymerase chain reaction

All procedures were performed with RNAse-free material and solutions. Tissue was lysed in 1 ml of TRIzol®, using 22G and 25G needles to shear DNA and fine-mince the sample. RNA was purified with RNeasy® Mini Kit columns (Cat: 74104, Qiagen) following the manufacturer's instructions. A spectrophotometer assessed RNA for concentration and quality by measuring optical density at wavelengths 260 and 280 nm. Samples were treated with DNAse (M610A) according to the manufacturer's instructions (Promega). RNA was reverse transcribed to cDNA using SuperScript™ II Reverse Transcriptase (Invitrogen). Forward and reverse primers to detect transcripts were purchased from Qiagen: aggrecan (QT00175364), neurocan (QT00158823), versican (QT00143220), with GAPDH as housekeeping control (QT01658692). Transcripts were quantified by real-time quantitative PCR on the iCycler (BioRad) using RT2 Real Time SYBR Green/Fluorescein PCR Master Mix (SA Biosciences). The relative expression levels between genes were calculated using a comparative cycle threshold method, with expression levels normalized to *GAPDH*.

Western blots

Lumbar spinal cord segments were used for western blots; after dissection from mice, tissue was flash frozen in liquid nitrogen, and stored in −80°C until processing. Tissue was sonicated in PBS on ice, then a solution of PBS, containing a protease inhibitor cocktail (cOmplete™ ULTRA Tablets, Roche) and phosphatase inhibitor cocktail (PhosSTOP™, Roche), was added to the tissues, and was left to shake at 4°C for 2 h. The solution was centrifuged at 12 500rpm for 15 min at 4°C. Supernatant was collected and protein was quantified with a bicinchoninic acid assay. Primary antibodies to CSPG core proteins required samples to be pretreated with 0.2 U/ml chondroitinase ABC overnight at 37°C prior to boiling with 4× sample buffer and running on SDS-PAGE. SDS-PAGE was run with a 3–8% Tris-acetate gradient gel (NuPAGE) for 1 h at a constant 150 V. Transfer was conducted with a nitrocellulose gel at a constant current of 125 mA at 4°C for 1.5 h. The blots were blocked with 10% skimmed milk for 1 h. All washes were conducted in Tris-buffered saline (TBS; 0.9% NaCl, 10 mM Tris-HCl, pH 7.5) containing 0.5% Tween 20 (TBS/Tween). Blots were incubated with primary antibodies in 3% skimmed milk overnight at 4°C. Primary antibodies used in this study are listed in Supplementary Table 1. The blots were then washed again before incubation with horseradish peroxidase-conjugated secondary antibodies. Bands were detected using an ECL chemiluminescence kit (GE Lifesciences) and manually exposing to developing and fixative solutions.

Band densities were quantified using Gel Analysis in ImageJ. A rectangular shape measured the density of bands for each lane. To compare the densities of bands between naïve and peak EAE, all bands were compared from the same gel image. Band densities were normalized to β-actin, to account for any loading control deviations.

Bone marrow-derived macrophages

Femurs were carefully removed from euthanized female C57Bl/6 mice, and marrow was flushed into a culture plate with cold complete bone marrow growth medium [Dulbecco's modified Eagle medium (DMEM), 10% foetal bovine serum (FBS), 2% penicillin/streptomycin and 10% supernatant from L929 cell-line enriched in macrophage-colony stimulating factor]. Cells were spun at 1100 rpm for 10 min, resuspended in fresh growth medium and plated at 1.2×10^6 cells/ml in a 10 cm culture dish. Cells were grown in DMEM supplemented with L929 supernatant for 5 days, then half the medium was replaced with fresh growth medium. On Day 7 growth medium was replaced with DMEM with 10% FBS. Cells were used on Day 8, and experiments were conducted in DMEM with 1% FBS unless otherwise specified.

TNFα ELISA and MMP luminex

Bone marrow-derived macrophages were plated at 50 000 cells in 96-well plates, and treated with 10 µg/ml CSPGs (Millipore C1177-K) or 100 ng/ml lipopolysaccharide (LPS) for 24 h. Media was taken for mouse cytokine/chemokine 31-plex discovery assay and multiplex MMP luminex (Eve Technology), which were performed according to manufacturer instructions.

Boyden chamber migration

Bone marrow-derived macrophages were plated in an uncoated filter insert with 8 µm pores at 500 000/filter in DMEM with 1% FBS. The lower well contained DMEM with 10% FBS as the high serum content served as a chemotactic stimulus. Treatments were added in the top filter in conjunction with the bone marrow-derived macrophages: 10 µg/ml CSPGs, 100 ng/ml LPS or media only as control. Transwell filters were 8 µm and uncoated polycarbonate (Corning costar transwell inserts, Cat#3422) or Matrigel®-coated (Corning Matrigel Invasion Chamber, Cat#354480). Following migration, the remaining cells on the top filter were washed off, and filters were fixed in cold acid alcohol for 30 min. Filters were washed again in PBS before staining in haematoxylin solution for 15 min and then placed on a coverslip. Cells were counted in 20× objective lens fields, vertically spanning the centre plane of the filter, excluding the areas at the top and bottom edges of the filter. The number of cells migrated per 20× field were averaged for each filter.

Statistical analysis

Before conducting a parametric test, datasets were tested for normal distribution with the D'Agostino-Pearson omnibus test ($P > 0.05$). When the sample set was small ($n < 10$), the Shapiro-Wilk normality test ($P > 0.05$) was used. Where multiple groups were compared, a one-way ANOVA with Tukey-Kramer's *post hoc* test for multiple comparisons was used. If the multiple comparisons were against a control group, a Dunnett's *post hoc* test was used. For comparisons between two groups, two-tailed Student's *t*-test was applied. $P < 0.05$ was considered statistically significant. All the statistical analyses were performed with Prism 6.0 software (GraphPad).

Results

CSPG members are altered in the inflamed spinal cord during EAE

We began with a time-course study to analyse changes of CSPGs by real-time PCR and western blots. The time points were chosen based on expected outcomes from previous experiments: onset of clinical signs (limp tail) at Day 12 following immunization, peak clinical severity (paresis/paralysis of all four limbs) at Day 18, and remission with residual deficits around Day 32 (Fig. 1A). The presence of inflammation in the spinal cord was corroborated by the progressive elevation of *Tnf* (TNFα) and *Tgfb1* (TGFβ) transcripts from preclinical samples to a maximum in specimens from mice at peak clinical EAE severity (Fig. 1B and C). Haematoxylin/eosin and Luxol fast blue staining of tissue and myelin integrity, respectively, were used to corroborate EAE neuropathology. The histological severity complemented the changes in clinical score, with a progressive increase in first pial and then parenchymal inflammation at peak clinical severity (Day 18) that was maintained at the chronic time point (Day 32) (Fig. 1D and E).

We investigated changes in transcripts for aggrecan (*Acan*), neurocan (*Ncan*) and versican (*Vcan*), the lectican CSPGs reported to be upregulated in active multiple sclerosis lesions (Sobel and Ahmed, 2001). The transcripts for the core proteins of aggrecan and neurocan in the spinal cord did not change significantly over the course of EAE but transcripts for total isoforms of versican were significantly elevated at peak clinical signs of EAE (Fig. 1F).

Selected enzymes that affect CSPG synthesis were also assessed by real-time PCR but were not altered during EAE (Supplementary Fig. 1A–C) and included: chondroitin sulfate N-acetylgalactosaminyltransferase 1 (CSGALNACT1), an enzyme in the early synthesis of the glycosaminoglycan of CSPGs; chondroitin 6-*O* sulfotransferase 1 (CHST3), an enzyme involved in post-translational sulfation of glycosaminoglycans; and exostosin glycosyltransferase 1 (EXT1), an enzyme involved in diverting synthesis towards heparan sulfate proteoglycans (HSPGs).

To corroborate the transcript findings, changes of CSPGs in the spinal cord of mice at peak clinical severity were analysed at the protein level with western blot. An antibody to intact 4-sulfated CSPG side chains, CSA, showed a prominent upregulation of glycosaminoglycan side chains in EAE versus naïve mice (Fig. 1G). The pixel density of bands in a group of mice, normalized to β-actin (Fig. 1H), was 1.9-fold increased for CSA in EAE mice at peak clinical severity versus naïve. In contrast to the lack of change in transcripts, western blot showed an elevation of aggrecan (1.7-fold) and brevican (1.5-fold). The versican V2 isoform decreased in EAE compared to naïve controls, whereas the versican V1 isoform was elevated in three mice (6.4-fold) (Fig. 1H). GFAP content was upregulated in EAE versus control (data not shown). Overall, these results highlight the substantial alterations of lectican CSPG members during EAE.

Versican V1 is upregulated in areas of inflammation in the spinal cord

Next, we localized the expression of CSPGs by immunohistochemistry, first using longitudinal sections of the spinal cord to allow a large area to be evaluated. Versican V1 immunoreactivity in the spinal cord was present as punctate staining in the grey matter in naïve mice (Fig. 2A and D) but its expression was highly prominent in meningeal (subpial) and parenchymal regions in EAE (Fig. 2B); meningeal inflammation has been previously reported in EAE by others and by us (Goncalves DaSilva and Yong, 2009) and it often precedes parenchymal inflammation (Goncalves DaSilva and Yong, 2009).

We observed versican V2 expression in both white matter and the grey matter. White matter expression of versican V2 was consistent with previous studies showing its localization along myelinated fibres at nodes of Ranvier (Dours-Zimmermann *et al.*, 2009) (Supplementary Fig. 2A). We

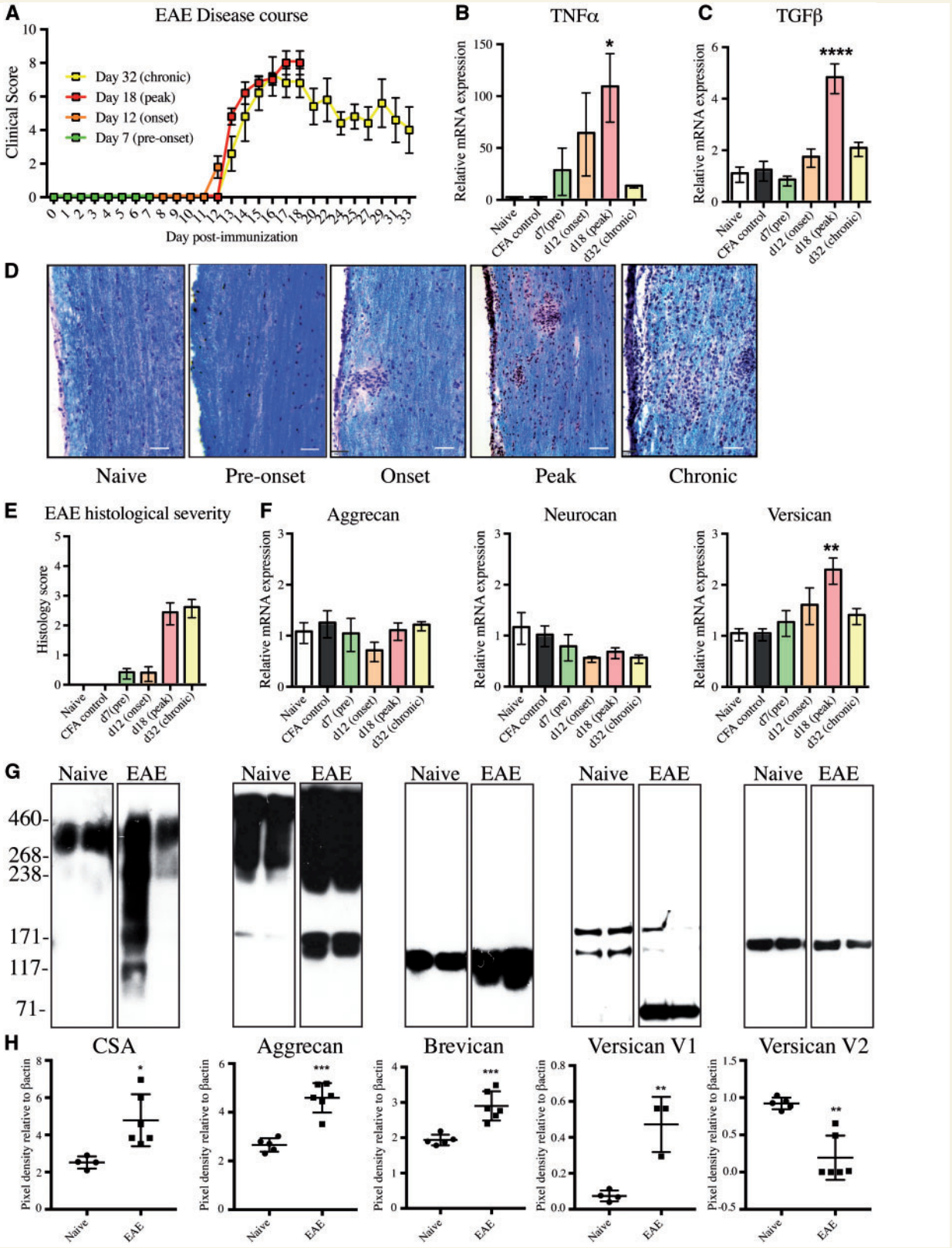

Figure 1 CSPGs are upregulated in the CNS of mice at peak EAE disease course. (**A**) Daily average EAE clinical score to Day 32. Day 0–12: pre-onset of clinical signs; Day 12: onset of clinical signs; Day 18: peak severity of clinical signs and > Day 18: chronic EAE. (**B** and **C**) Real-time PCR showing the upregulation of *Tnfa* (TNFα) and *Tgfb1* (TGFβ) at peak EAE. For panels **A–C**, values are mean ± SEM of five mice. (**D**) Haematoxylin, eosin and Luxol fast blue staining (H&E/LFB) shows the presence of pial inflammation of the spinal cord at the onset of EAE, progressing to parenchymal lesions at both peak and chronic time points. Scale bars = 50 μm. (**E**) Histological severity scoring of the H&E/LFB staining, analysed by the degree and location (pial versus parenchymal) of inflammatory infiltrates. (**F**) Real-time PCR of the lectican CSPGs

(continued)

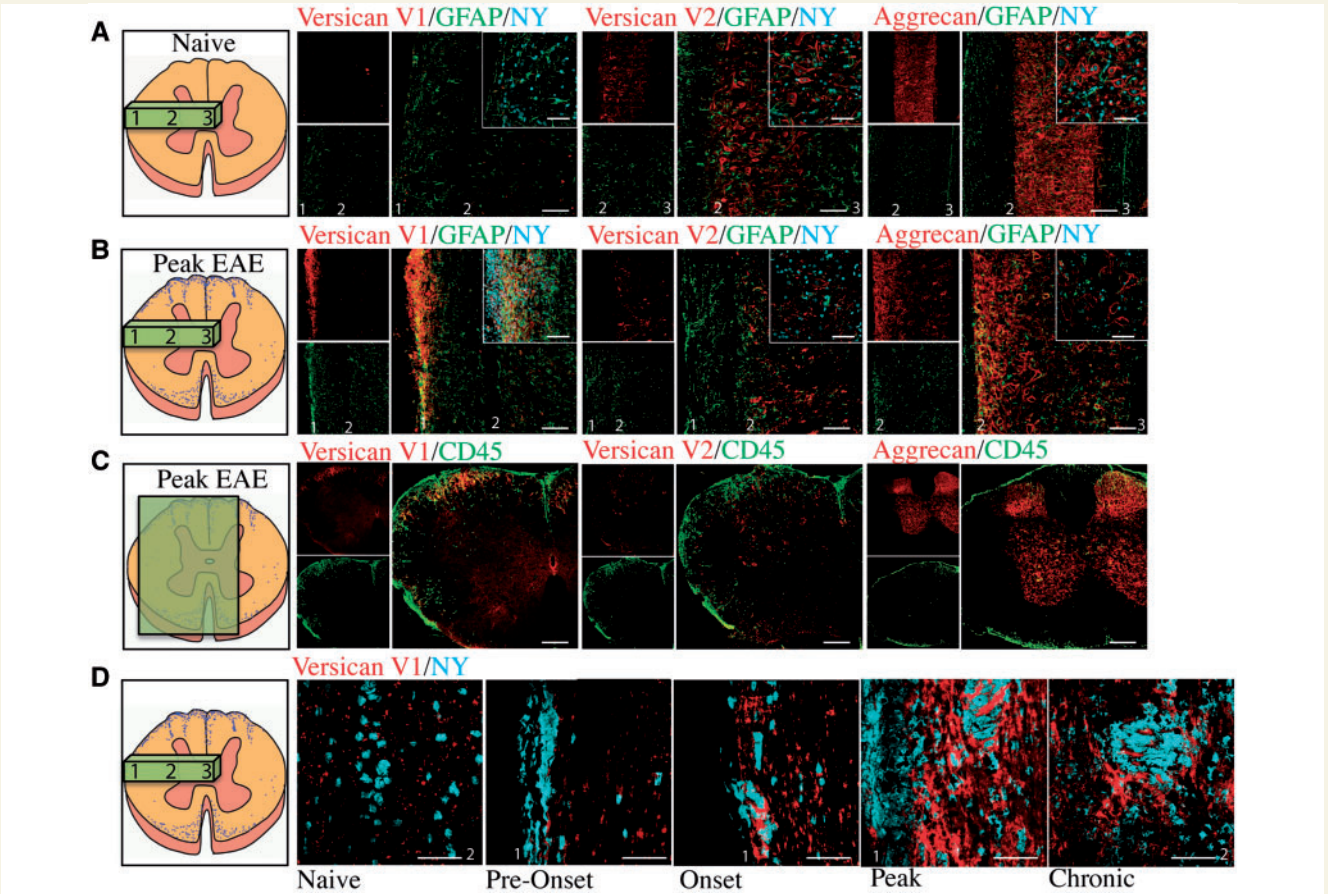

Figure 2 Versican V1 expression is upregulated at peak EAE correspondent with regions of inflammation. Longitudinal sections of versican V1, versican V2, and aggrecan (red) co-stained with GFAP (green) and nuclear yellow (NY, blue) in (**A**) naïve mice and (**B**) EAE mice at peak disease severity; we used GFAP as an indicator of the response of CNS-intrinsic cells during EAE. (**C**) Versican V1, versican V2, and aggrecan (red) staining shows that V1 was correspondent with CD45+ (green) cells in coronal spinal cord sections from EAE mice; conversely, V2 and aggrecan were not upregulated in regions of inflammation. (**D**) Versican V1 (red) staining in the mouse EAE thoracic spinal cord at naïve (non-immunized), pre-onset, onset, peak, and chronic time points co-stained with nuclear yellow (NY, blue) as a nuclear marker. Spinal cord schematics on the far left show the slice orientation, and numbers that correspond to pial region (1), grey matter boundary (2) and centre of the spinal cord (3), that are labelled in the immunohistochemistry images. *Insets* show higher magnification. Scale bars = 50 μm.

also observed versican V2 expression in perineuronal nets (Carulli *et al.*, 2006) in both naïve and peak EAE spinal cords (Fig. 2A, B and Supplementary Fig. 2B). We found aggrecan expression confined to the grey matter, abundantly expressed in perineuronal net structures that surrounded NeuN-positive neurons (Supplementary Fig. 2C). Aggrecan was expressed solely in the grey matter, in both naïve mice and at peak EAE (Fig. 2A and B).

We then examined the localization of CSPGs in coronal sections, to corroborate expression correspondent with areas of CD45+ infiltrating leucocytes. Versican V1 was highly expressed where CD45+ leucocytes were infiltrating

Figure 1 Continued

aggrecan (*Acan*), neurocan (*Ncan*), and total isoforms of versican (*Vcan*) (V0, V1, V2, V3). For panels **E** and **F**, values are mean ± SEM of five mice. For panels **B**, **C**, **E** and **F**, datasets passed the Shapiro-Wilk normality test and Dunnett's ANOVA was performed, comparing immunized mice groups against naïve, $*P < 0.05$, $**P < 0.01$, $***P < 0.001$, $****P < 0.0001$. (**G**) Western blot of spinal cord samples from naïve and peak EAE mice (two mice represented/condition) of CSPGs including chondroitin sulfate 4-sulfated glycosaminoglycan chains (CSA), aggrecan, brevican, versican V1/V0, and Versican V2/V0. The presence of lower molecular weight protein cores of aggrecan, brevican, and versican V1 likely represent cleavage from matrix-metalloproteinases or a disintegrin and metalloproteinase with thrombospondin motifs (ADAMTs) within the samples. (**H**) Relative changes of the density of bands in peak EAE compared to the density of bands in naïve mice. Densities of the bands were normalized to β-actin as a loading control. Chondroitin sulfate A (CSA), aggrecan, brevican and versican V1 datasets passed the Shapiro-Wilk normality test, and a two-tailed Student's *t*-test showed significant increases in peak EAE versus naïve mice ($*P < 0.05$, $**P < 0.01$, $***P < 0.001$). Versican V2 did not pass normality, and the non-parametric two-tailed Mann-Whitney test showed a significant decrease in versican V2. Each square represents a separate mouse spinal cord. CFA = complete Freund's adjuvant.

from meningeal regions (Fig. 2C). Neither versican V2 nor aggrecan were highly expressed in regions of CD45+ infiltration (Fig. 2C). A time course analysis of versican V1 expression showed that the punctate staining of versican in the white matter in naïve and early time points of EAE was significantly upregulated as EAE severity progressed, most prominently at peak (Fig. 2D).

CSPGs are upregulated in perivascular cuffs in EAE spinal cord

In this study we chose to focus on perivascular cuffs due to the possibility that the perivascular cuff act as a regulatory checkpoint, with the accumulated immune cells requiring a second enhancing stimulus prior to crossing the glial limitans/parenchymal basement membrane (Tran *et al.*, 1998; Archambault *et al.*, 2005; Agrawal *et al.*, 2006; Engelhardt, 2006; Toft-Hansen *et al.*, 2006; Owens *et al.*, 2008). Perivascular cuffs can be visualized with a pan-laminin antibody to highlight both basement membranes, and CD45 to label immune cells (Fig. 3A). Perivascular cuffs are not detected in the CNS of control mice or presymptomatic mice but they become visible and increasing in number with EAE progression (Agrawal *et al.*, 2013). In our previous work, leucocyte populations within perivascular cuffs include CD3+ T lymphocytes, CD20+ B cells and CD68+ monocyte/macrophages (Agrawal *et al.*, 2013). In the EAE mice analysed in this study, monocyte/macrophage-like cells constituted the majority of cells in the perivascular cuffs (~80%) whereas a second abundant cell type, CD3+ T

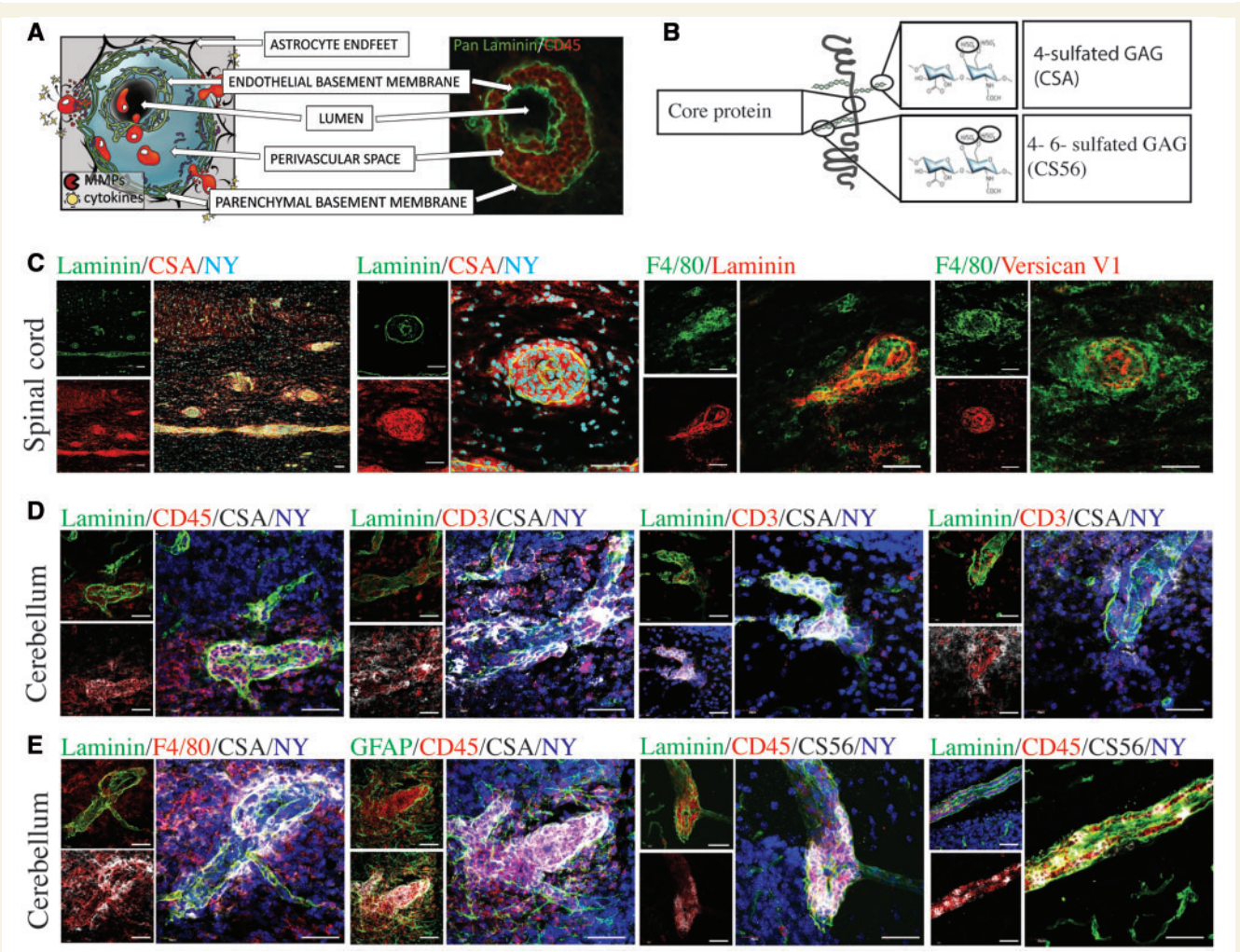

Figure 3 CSPGs are expressed in perivascular cuffs. (**A**) An inflammatory perivascular cuff schematic and cuff from an EAE mouse, depicted with CD45-positive cells (red) accumulated in the perivascular space between the endothelial and the parenchymal basement membranes, visualized by pan-laminin (green). (**B**) Schematic to illustrate the structure specificity of CSPG antibodies, including the versican core protein, the antibody to 4-sulfated chondroitin sulfate glycosaminoglycans (CSA) and 4-sulfated or 6-sulfated chondroitin sulfate glycosaminoglycans (CS56). (**C**) Perivascular cuffs in the spinal cord depicted with pan-laminin (green) as well as F4/80 (green), and the CSPG stains CSA and versican V1 (red). (**D**) Perivascular cuffs in the cerebellum stained with pan-laminin (green) and nuclei (nuclear yellow, NY, blue) showing CSA (white) staining associated with infiltrating CD45+ and CD3+ cells (red). (**E**) Perivascular cuffs in the cerebellum showing the relationship of CSA and CS56 (white) to astrocytes (GFAP, green), macrophages/microglia (F4/80, red), and the perivascular cuff (pan-laminin, green). Scale bars = 50 μm.

lymphocytes, represented approximately 15% (Supplementary Fig. 3A and B). Although multiple sclerosis tissue specimens showed greater variability in the representation of macrophages (CD68+) and CD3+ cells in the cuff (Supplementary Fig. 3C and D), CD68+ cells were an abundant cell type. However, the relative proportion of leucocyte subsets can vary across cuffs, likely reflecting disease activity, stage of evolution of a particular cuff, or simply randomness.

We found that the perivascular cuffs were also highly abundant for CSPG expression. Antibodies used identified the core protein versican V1, the 4-sulfated CSPG glycosaminoglycan side chains (CSA), and the 4- and 6-sulfated CSPG glycosaminoglycans (CS56) (Fig. 3B). We began with the thoracic spinal cord, a region highly affected by the ascending inflammation that progresses into higher brain regions. In these spinal cord samples, the antibody to intact 4-sulfated CSPG side chains (CSA) revealed significant staining within the double membranes of perivascular cuffs (Fig. 3C). As the versican antibody used was raised in rabbit, we were unable to use it simultaneously with the rabbit anti-pan laminins. A perivascular cuff stained with F4/80 showed abundant F4/80+ monocytes/macrophages with interspersed versican V1 expression (Fig. 3C).

In previous work, we found that the cerebellum during EAE presents with clearly identifiable perivascular cuffs, commonly confined to the white matter tracts (Agrawal *et al.*, 2013). Thus, to localize CSPGs better, we investigated the cerebellum and visualized CSA staining brightly in the perivascular space with accumulated CD45+ leucocytes, CD3+ T lymphocytes and F4/80+ macrophages (Fig. 3D and E). Following extravasation of leucocytes, CSA was still observed in the perivascular space, with reduced intensity, but now appeared in the parenchyma in regions of extravasated leucocytes (Fig. 3D and E).

A second antibody that visualizes CSPG side chains is CS56, which is specific for intact 4- and 6-sulfated glycosaminoglycan side chains (Fig. 3B). CS56 was also present in the perivascular cuff, associated with accumulated immune cells (Fig. 3E).

CSPGs have been shown to bind several molecules that may also serve as their receptors, including selectins, toll-like receptors, integrins, and CD44 (Kawashima *et al.*, 2000, 2002; Zheng *et al.*, 2004; Kim *et al.*, 2009). We stained for the presence of one of these, CD44, and found that leucocytes expressed CD44 within the perivascular cuff (Supplementary Fig. 4). Thus, these leucocytes have the capacity to produce CSPGs that in turn can act back on themselves through the engagement of CD44.

The source of versican V1 in perivascular cuffs

Because of the abundant expression of CSPGs in perivascular cuffs, it was difficult to describe their precise association with immune cells. We thus used surface rendering with the Imaris program to better investigate the 3D association of immune cells in cuffs (Fig. 4A) and of CSPGs with immune cells. Surface rendering of *z*-stacks of CD45 and versican V1 staining clearly demonstrate the localization of versican V1 staining within CD45+ cells and extracellularly in proximity to these cells (Fig. 4B). Surface rendering showed that versican V1 was also closely associated with PDGFRβ+ cells (Fig. 4C), which may represent its association with pericytes, meningeal fibroblasts, or astrocytes (Lindahl *et al.*, 1997). CSA was associated with both CD45+ cells and GFAP+ astrocyte endfeet that contact the parenchymal basement membrane (Fig. 4D).

To establish the versican V1 associated with CD45+ cells within perivascular cuffs could indeed be produced by these leucocytes, we designed a probe to detect the versican V1 transcript through *in situ* hybridization studies. In the EAE spinal cord the versican V1 transcript was detected in CD45+ leucocytes and F4/80+ monocytes/macrophages (Fig. 4E).

Overall, these studies show that versican V1 and CSA immunoreactivity are intimately associated with leucocytes during their transit within the perivascular cuff and as they migrate into the CNS parenchyma.

CSPGs enhance the production of matrix metalloproteinases and transmigratory capacity of macrophages

The correspondence of infiltrating leucocytes and CSPGs suggest their potential to regulate one another. To extravasate out of the perivascular space and through the glial limitans/parenchymal basement membrane, leucocytes must produce extracellular matrix-degrading proteases such as the matrix metalloproteinases (MMPs) (Yong, 2005; Gerwien *et al.*, 2016). We thus tested the hypothesis that CSPGs in perivascular cuffs facilitate the activation and trafficking of leucocytes. Since macrophages are highly abundant within perivascular cuffs (Fig. 3 and Supplementary Fig. 3), we evaluated bone marrow-derived macrophages in tissue culture studies. Because of the lack of commercial V1 from mammalian sources, we used a CSPG mixture abundant in versican, but also containing the lecticans aggrecan and neurocan.

Macrophages treated with the CSPG mixture significantly upregulated the production of 14 of the 31 molecules within a cytokine/chemokine multiplex set. Inflammatory cytokines that were significantly enhanced by CSPGs included: granulocyte-colony stimulating factor (G-CSF), granulocyte-macrophage colony stimulating factor (GM-CSF), interleukin (IL)-6, IL-5, IL-1α, IL-1β, and tumour necrosis factor-α (TNFα) (Fig. 5A and Supplementary Fig. 5). Chemokines were also enhanced, including: chemokine (C-C) motif 2, 3, 4, 5, and chemokine (C-X-C) motif 1, 2, 10 (Fig. 5B and Supplementary Fig. 5).

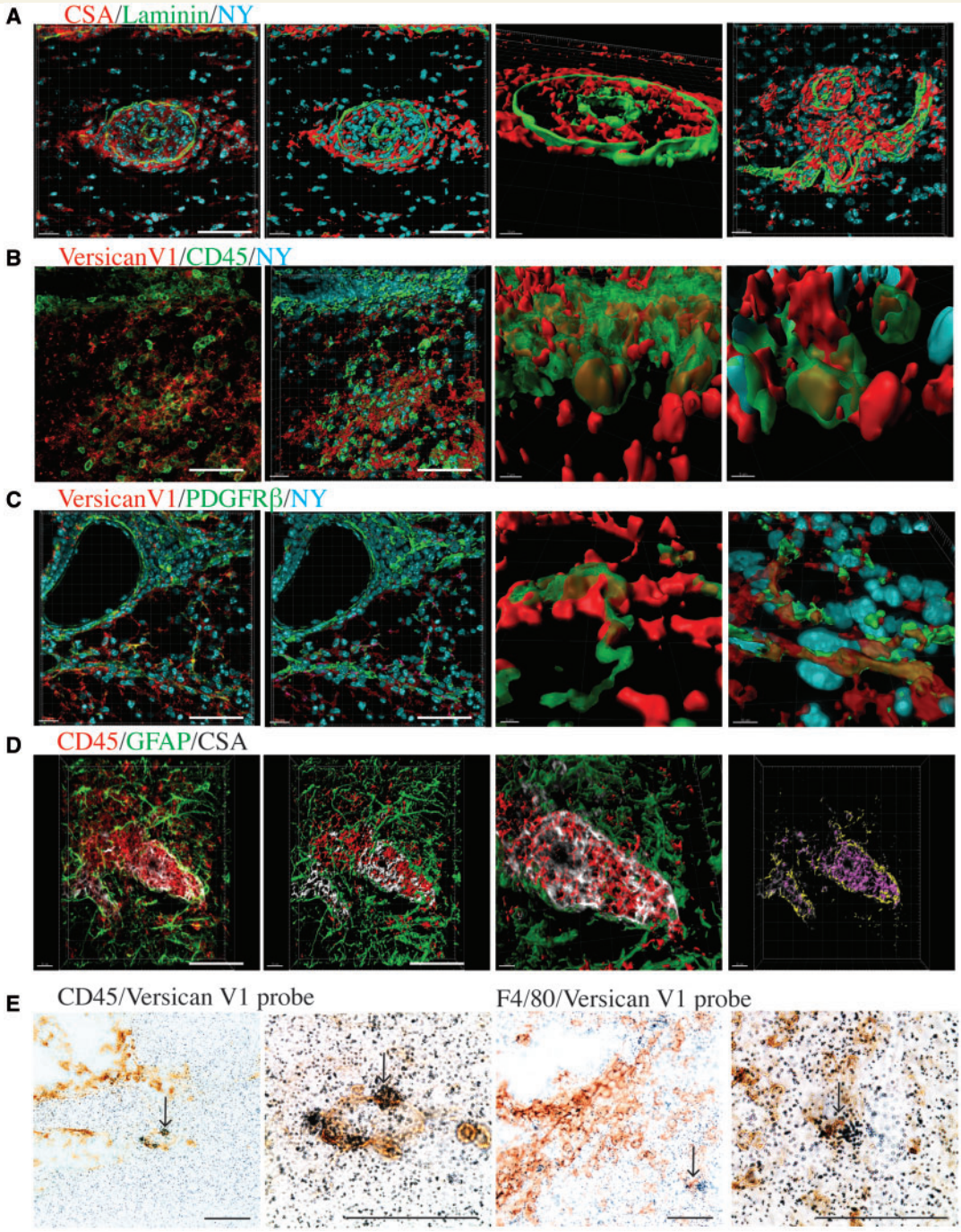

Figure 4 Cellular associations of versican V1 staining in regions of cuffs. (**A**). From *left* to *right*, (1) an unedited image of a perivascular cuff in the spinal cord with CSA (red) with pan-laminin (green), and nuclear yellow (NY), next to (2) an Imaris-generated surface rendering. (3) An alternative viewpoint of the surface rendered perivascular cuff, showing CSA within the pan-laminin cuff. (4) A second example of a surface rendered perivascular cuff. (**B**) From *left* to *right*, (1) Versican V1 (red)/CD45 (green)/nuclear yellow (NY, blue) with original staining next to (2) the surface rendering of CD45+ cells. (3 and 4) Two magnified images showing versican V1 staining within and surrounding CD45+ cells. (**C**) From *left* to *right*, (1) original image of PGFRβ staining (green) in conjunction with versican V1 (red), and a nuclear dye (nuclear yellow, NY, blue), and (2) surface rendering. (3 and 4) Two magnified images show the association of versican V1 with PGFRβ+ cells. (**D**) From *left* to *right* (1) original image of CD45 (red), GFAP (green), and CSA (white) staining of a perivascular cuff in the cerebellum and (2) the surface rendering. (3) Magnification of the perivascular cuff, with surface rendering of GFAP and CD45 staining, and original CSA staining. (4) Correspondence of CSA with GFAP (yellow overlap) and of CSA with CD45 (pink) showing CSA localization with astrocyte endfeet and immune cells in the perivascular cuff. Scale bars (*bottom right*) = 50 μm; program-generated scale bars on the *bottom left* specify length. (**E**) *In situ* hybridization of versican V1. From *left* to *right*, (1) CD45+ cells in a cuff-like structure, and (2) magnified image, where the cluster of silver grains around a CD45+ cell is indicative of transcript expression for versican V1 by leucocytes. Arrow locates the same cell in the low and higher magnified image. (3) F4/80+ infiltrating cells in a cuff-like structure and (4) magnified image. Arrow locates the same cell in the low and higher magnified image. Scale bars = 50 μm.

Macrophages were treated with the CSPG mixture and their secretion of several MMP members was evaluated through multiplex analysis of the conditioned media. LPS, a potent toll-like receptor activator of macrophages, was used as a robust activation control. Notably, CSPGs significantly enhanced production of several MMP members, including MMP-2, MMP-3, MMP-8, MMP-9 and MMP-12, beyond those of LPS-stimulated macrophages (Fig. 5C).

The capacity of CSPGs to elevate MMPs more potently than LPS, and the difference in cytokine upregulation by LPS and CSPGs, reduces the possibility that the CSPG effect was due to LPS contamination within the CSPG mixture. Nonetheless, to ensure that the effects of CSPGs were not due to LPS contamination, we incubated the CSPG mixture with polymyxin B, which has been shown to bind LPS and suppress LPS activity (Warren, 1982). CSPGs mixed with polymyxin B enhanced MMP-9 levels in macrophages to a similar extent as CSPGs alone (Supplementary Fig. 6). Thus, CSPGs are potent mediators of MMP elevation.

Given that the activity of MMPs contributes to the transmigration process (Yong, 2005; Sorokin, 2010), we then investigated whether CSPGs could enhance migration of macrophages using a two-compartment Boyden chamber assay; in this technique, cells seeded in the top chamber migrate across a filter containing pores of 8 μm diameter

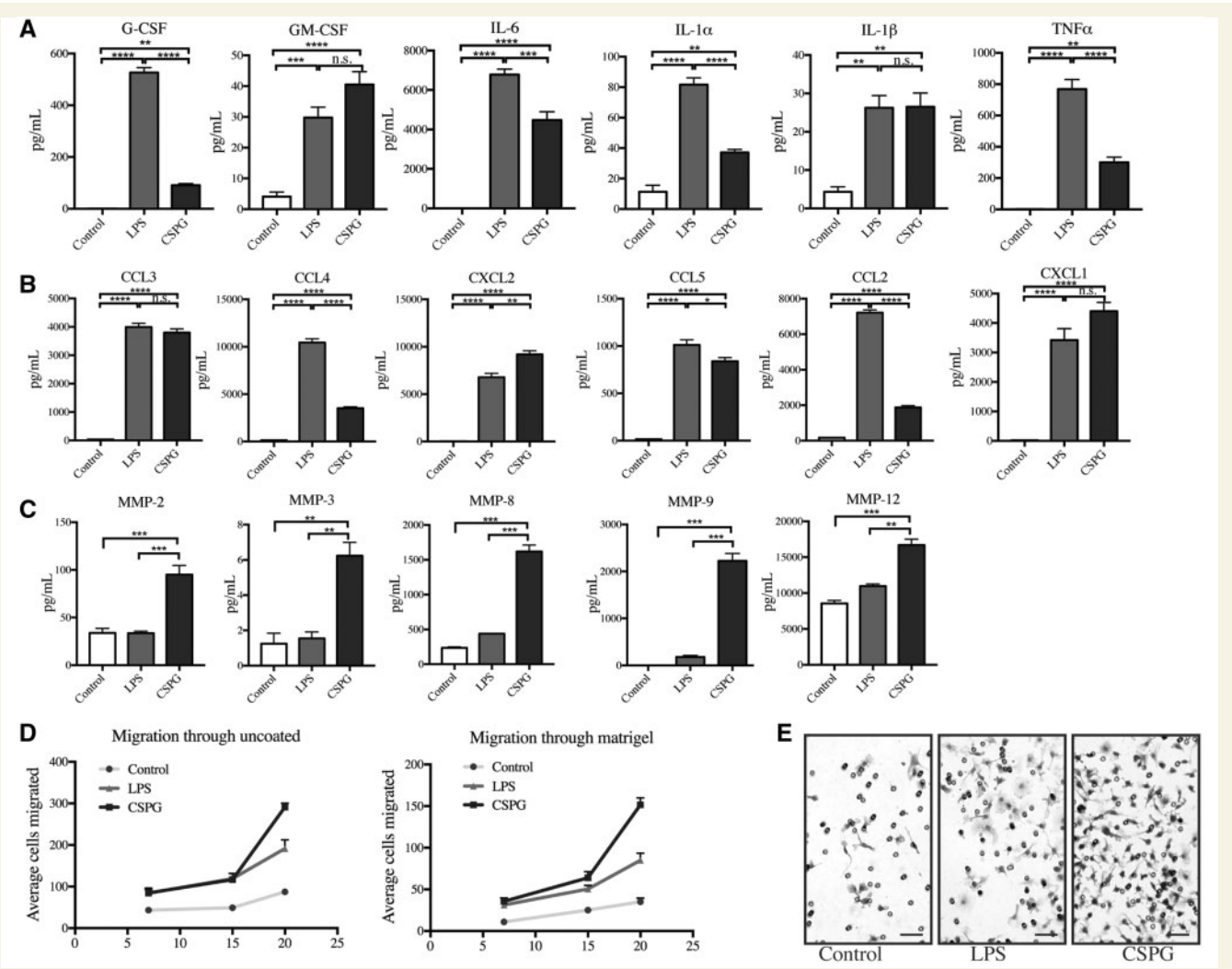

Figure 5 CSPGs enhance MMP production and migration of bone-marrow derived macrophages. Cytokine 31-plex assay in bone-marrow derived macrophages treated with media, LPS, or CSPGs for 24 h showing CSPGs significantly upregulate (**A**) cytokines and (**B**) chemokines. (**C**) MMP luminex shows that CSPGs significantly upregulate MMP-2, MMP-3, MMP-8, MMP-9, and MMP-12 beyond LPS stimulation of macrophages. (**D**) Boyden migration of macrophages through 8 μm uncoated and Matrigel-coated filters, treated with LPS or CSPGs, or media only. Average cells migrated in a ×20 field per filter at 7, 15, 20 h. (**E**) Example images of migrated macrophages at 20 h on the lower side of Matrigel-coated filters, stained by haematoxylin. Scale bars = 200 μm. Data represent mean ± SEM. For all experiments, macrophages were treated with 10 μg/ml CSPGs, 100 ng/ml LPS, and media only was used as a control. ANOVA with Tukey *post hoc* test was performed, comparing media, LPS, or CSPG treatments against each other. *$P < 0.05$, **$P < 0.01$, ***$P < 0.001$. n.s. = non-significant.

into the lower chamber containing chemoattractants (Radeke *et al.*, 2005; Agrawal *et al.*, 2013). We first assayed migration across an uncoated filter at 7, 15 and 20 h, and found that the addition of CSPGs to cells enhanced the migration of macrophages an average of 2.0-, 2.4-, and 3.3-fold, respectively (Fig. 5D and E). Next, and to recapitulate the basement membrane and the role of matrix-degrading enzymes, we used Boyden chambers where the filter was coated with Matrigel®, a commercially available extracellular matrix mixture secreted by Engelbreth-Holm-Swarm (EHS) mouse sarcoma cells. In Matrigel®-coated filters, fewer control cells migrated compared to uncoated filters. Nonetheless, transmigration in Matrigel®-coated wells was promoted by CSPGs (Fig. 5D and E) an average of 3.2-, 2.5-, and 4.3-fold at 7, 15, and 20 h, respectively. Through both uncoated and coated filters, CSPGs produced a more robust transmigration compared to LPS, which may be because of both the greater capacity of CSPGs to elevate MMPs relative to LPS, as well as other potential effects on macrophage activity as informed by the cytokine/chemokine elevation.

Targeting CSPGs to reduce perivascular cuffs and leucocyte infiltration

To understand the role of CSPGs in the ability of leucocytes to influence leucocyte migration further, we investigated whether pharmacological blockade of CSPGs influenced the number of CD45+ cells infiltrating the spinal cord from perivascular cuffs. Previous studies from our laboratory have shown that fluorosamine successfully reduced CSPG production *in vitro* and *in vivo*, and that its administration to mice at peak EAE clinical score significantly reduced *Vcan* (versican) mRNA in the spinal cord and attenuated subsequent EAE disease severity (Keough *et al.*, 2016). We examined spinal cords from those EAE mice, and found that the total number of CD45+ cells that had migrated past the parenchymal basement membrane were significantly lower in fluorosamine-treated mice than vehicle-treated controls (Fig. 6A). Within a 100 µm distance from cuffs, approximately half of CD45+ cells in fluorosamine-treated mice were clustered within the perivascular space, whereas less than 15% of CD45+ cells in vehicle-treated mice were retained in the perivascular space (Fig. 6B).

Versican expression in perivascular cuffs in multiple sclerosis samples

We next sought to investigate the expression of CSPGs in multiple sclerosis. We examined frozen CNS specimens from four patients with multiple sclerosis that we had predetermined to contain inflammatory perivascular cuffs in the white matter, visualized by pan-laminin and CD45+ staining (Fig. 7A). Adjacent sections were examined for expression of control or versican V1 staining. The absence of primary antibody showed a dim fluorescence around cuffs, and an isotype control used in place of the primary rabbit versican antibody was similarly negative (Supplementary Fig. 7A). In contrast, versican V1 immunoreactivity was prominent and restricted to cuff-like structures (Fig. 7B) for all four multiple sclerosis brain specimens. As with EAE, we found that versican V1 was closely associated with infiltrating immune cells, stained with CD45+ and CD3+ markers (Fig. 7C). In contrast, neurocan and versican V2 did not reveal staining in perivascular cuffs (Supplementary Fig. 7B and C). Finally, multiple sclerosis perivascular cuffs in all four multiple sclerosis brain specimens were also immunoreactive for chondroitin sulfate glycosaminoglycans (CSA) (Fig. 7D). Imaris rendered cuffs clearly show the expression of CSA within the perivascular space (Fig. 7E).

Discussion

We have demonstrated that in multiple sclerosis and EAE there is an upregulation of the lectican versican V1 and chondroitin sulfate glycosaminoglycans. Previous work has shown how CNS injuries such as spinal cord injury can cause increase of CSPGs (McKeon *et al.*, 1991; Davies *et al.*, 1996; Tang *et al.*, 2003; Jones *et al.*, 2005; Galtrey *et al.*, 2008). Moreover, Sobel and Ahmed (2001) reported that lectican CSPG members are elevated at the edge of expanding lesions in multiple sclerosis, and presumably also within lesions where they can be found within phagocytic macrophages.

Our study is the first on multiple sclerosis to investigate the in-depth changes of specific members of CSPGs. We found that in EAE, total *Vcan* (versican) transcripts were elevated, and versican V1 protein was significantly upregulated and expressed in pial regions of infiltrating CD45+ cells. In contrast, versican V2 protein was downregulated and not expressed in regions of pial inflammation. Aggrecan protein level was upregulated in peak EAE but its expression was confined to the grey matter, likely representing its continued incorporation in perineuronal nets. The increase in protein of versican V1 and decrease in versican V2, as well as the diverse spatial expression of CSPG members further emphasizes the different regulatory mechanisms, cellular sources, and consequences of CSPG member upregulation; future studies need to distinguish between CSPG members to understand their distinct roles in CNS pathology.

We also described the novel finding that versican V1 and CSA (4-sulfated glycosaminoglycans) are upregulated in the perivascular space, and closely associated with infiltrating immune cells in both EAE and multiple sclerosis. Moreover, the presence of CD44, a receptor for CSPGs, suggests the potential for CSPGs to directly affect leucocyte activity. *In situ* hybridization identified versican V1 transcripts in CD45+, and F4/80+ cells. These findings

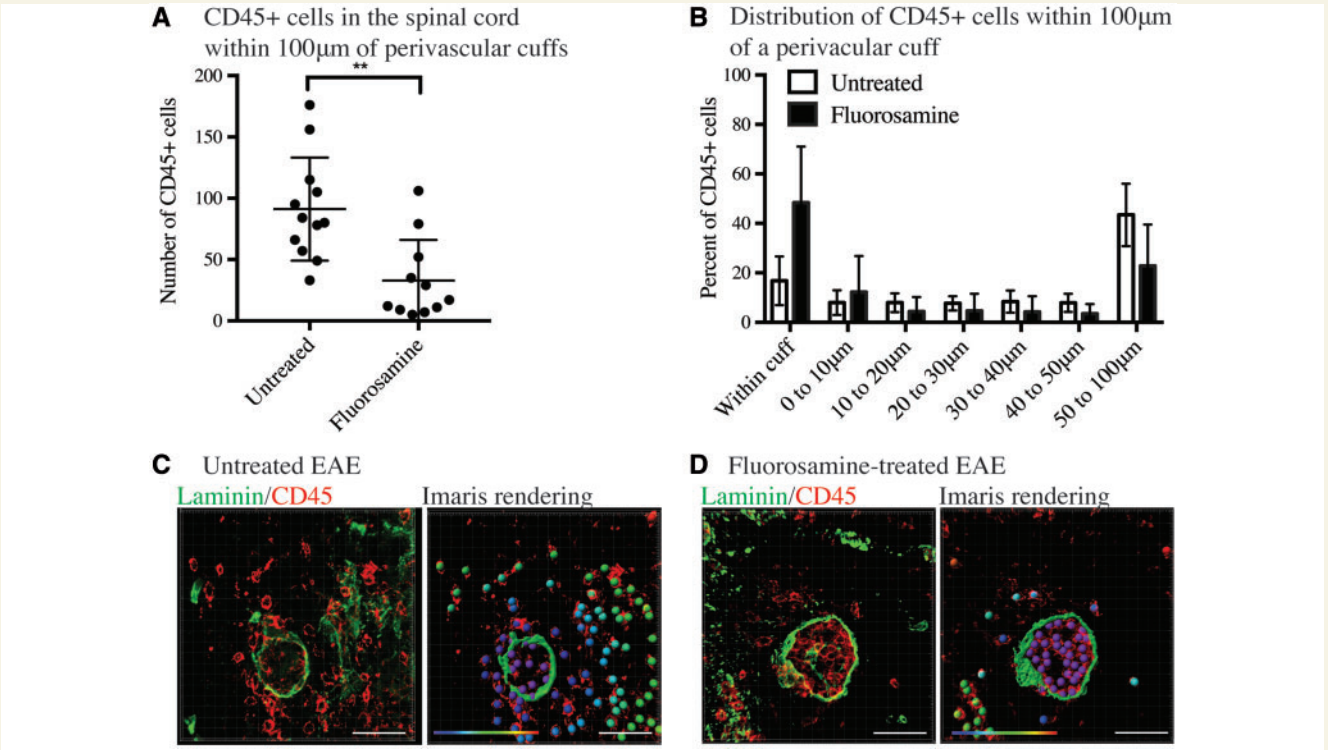

Figure 6 Targeting CSPGs with fluorosamine reduces the infiltration of CD45 + cells into the spinal cord parenchyma. (**A**) CD45 + cells were stained by immunohistochemistry and rendered as 'spots' in Imaris. Imaris quantified the number of CD45 + cells in the spinal cord 100 μm from perivascular cuffs (identified with pan-laminin staining). CD45 + cells within the perivascular cuff were not included in this analysis. (**B**) Distribution of CD45 + cells within 100 μm of perivascular cuffs in fluorosamine-treated and untreated EAE spinal cords. (**C**) *Left*, immunohistochemistry of a perivascular cuff in an untreated mouse and *right*, Imaris rendering of laminin staining as a surface and CD45 + as spots overlain on true CD45 + (red) staining. Distance of CD45 + cells from the perivascular cuff is represented in their colour gradient (shown in the *bottom left*), with purple representing nearby and red far. (**D**) *Left*, immunohistochemistry of a perivascular cuff of fluorosamine-treated EAE mouse. *Right*, Imaris rendering of laminin as a surface and CD45 + as coloured spots, overlain on true CD45 + (red) staining. Distance of CD45 + cells from the perivascular cuff is represented in their colour gradient (shown in the *bottom left*), with purple representing nearby and red far. Spinal cords from four mice in each group were quantified. Scale bars = 50 μm.

corroborate previous results that have shown that both monocytes and peripheral blood mononuclear cells increase chondroitin sulfate glycosaminoglycan production following pro-inflammatory stimuli (Kolset *et al.*, 1983; Levitt and Ho, 1983; Uhlin-Hansen *et al.*, 1989). Versican V1 in particular is upregulated in infiltrating proinflammatory subtypes of macrophages and monocytes (Toeda *et al.*, 2005; Martinez *et al.*, 2006). However, other cell types may also be responsible for CSPG production within the CNS, including astrocytes, oligodendrocytes, endothelial cells, and pericytes. As well, another source of CSPGs may be from serum leakage through a compromised blood–brain barrier.

To investigate the potential consequences for CSPG upregulation, we used tissue culture experiments and also investigated the consequences of a pharmacological blockade of CSPGs in mice. We found that functional consequences of CSPGs *in vitro* included the enhanced upregulation of pro-inflammatory cytokines, chemokines and MMPs. Due to the requirement of MMPs to migrate through the second parenchymal border, we tested whether CSPGs could enhance the mobility of macrophages. Indeed, CSPGs promoted the migration of macrophages as much as 4-fold through Matrigel®-coated filters.

Mice with EAE that were treated with fluorosamine, a CSPG-lowering compound, have reduced EAE clinical score and *Vcan* mRNA (Keough, 2016). The spinal cords of fluorosamine-treated animals had reduced number of CD45 + cells in the parenchyma in the vicinity of cuffs, compared to untreated mice. A higher proportion of CD45 + cells were clustered within the perivascular space in fluorosamine treated mice, versus infiltrated into the surrounding parenchyma. There are undoubtedly multiple factors that influence leucocyte infiltration into the CNS; our results suggest that the CSPG versican may be one factor involved in promoting leucocyte migration into the CNS. This is corroborated by the use of fluorosamine, a CSPG-lowering compound that reduces the number of CD45 + cells that exit a perivascular cuff to migrate deep into the CNS parenchyma.

Versican belongs to the lectican family of CSPGs, and is widely distributed throughout the body in adult tissues, and is highly expressed in developing white matter tracts where

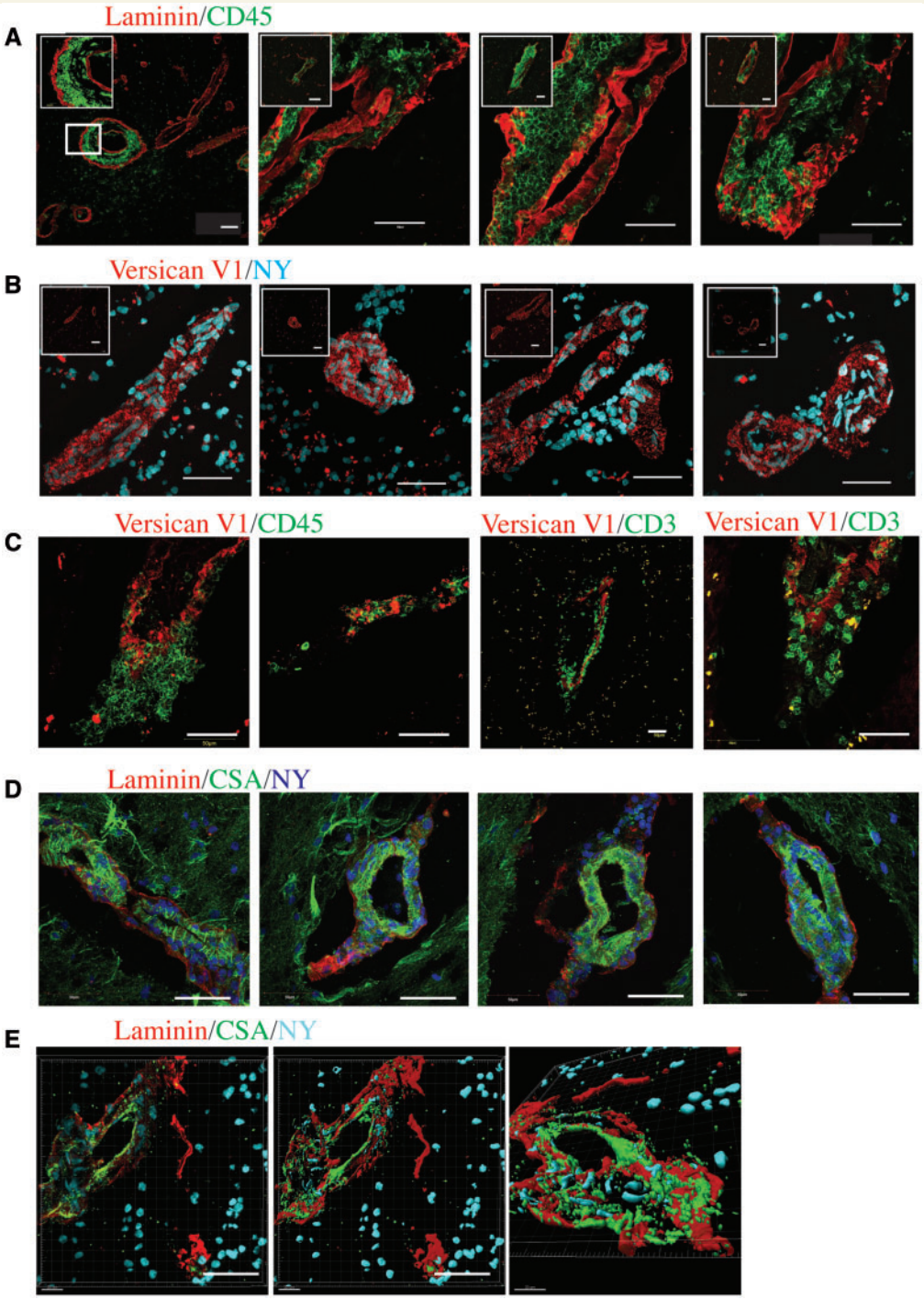

Figure 7 Versican is present in perivascular cuffs in multiple sclerosis brain tissue. (**A**) Pan-laminin (red) and CD45 (green) staining showing examples of perivascular cuffs throughout the parenchyma of multiple sclerosis brains. *Leftmost insert* shows a magnified image, whereas the remaining inserts show a lower magnification of the cuffs. (**B**) Versican staining (red), with a nuclear dye (nuclear yellow, NY, blue) present in numerous perivascular cuff-like structures throughout multiple sclerosis brain tissue. *Insets* show lower magnification of the cuff. (**C**) Versican V1 (red) staining in perivascular cuffs with CD45 + or CD3 + (green) infiltrating immune cells. (**D**) CSA (green) within endothelial and parenchymal basement membranes (pan-laminin, red), showing chondroitin sulfate glycosaminoglycans within the cuffs with accumulated cells (nuclear yellow, NY, blue). (**E**) Imaris rendering of a perivascular cuff, stained with CSA (green) and pan-laminin (red) to show the presence of chondroitin sulfate glycosaminoglycans within the perivascular space. *Far left* shows the original image, next to a surface rendering, and a new viewpoint (*far right*). Scale bars = 50 μm.

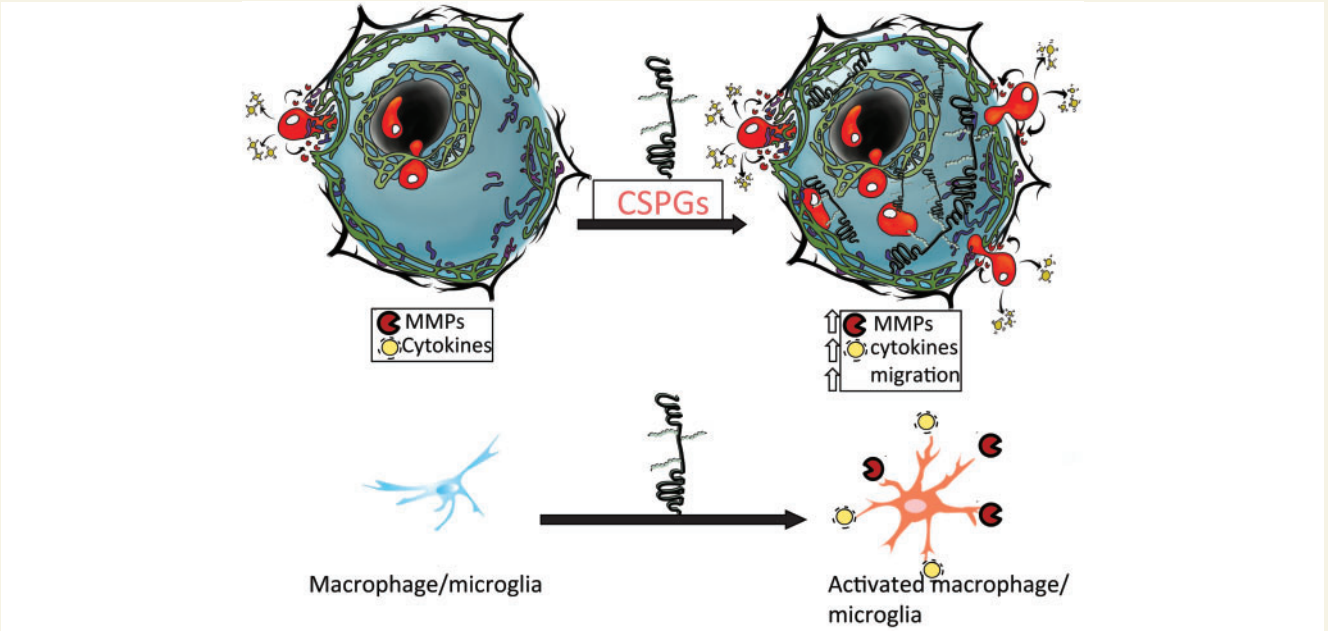

Figure 8 Schematic that illustrates that CSPGs are present in the perivascular space, and are able to enhance the production of pro-inflammatory cytokines and MMPs, promote migration, and thus contribute to infiltration of immune cells into the CNS.

it is known to have roles in development migration and myelination (Bignami *et al.*, 1993; Landolt *et al.*, 1995; Dutt *et al.*, 2006). The upregulation of versican during a variety of insults point to its role as a versatile player in injury and inflammation. Lessons from non-CNS conditions point to the roles of CSPGs, and in particular versican, as a driver of inflammation. In lung inflammation, hyaluronan-versican interactions are important for immune cell recruitment, and conditional knock-out of versican reduced lung inflammation, infiltration of leucocytes, and levels of pro-inflammatory cytokines (Kang *et al.*, 2017). Versican purified from Lewis lung carcinoma promoted the production of pro-inflammatory cytokines such as TNFα, IL-1β, and IL-6 on macrophages, endothelial cells, and fibroblasts (Kim *et al.*, 2009). In summary (Fig. 8), we have found several novel aspects of how CSPGs are altered in EAE and multiple sclerosis, and how CSPGs can shape cell responses by enhancing pro-inflammatory cytokine release, MMP production, and migration. An additional novelty is the upregulation of versican V1 in inflammatory perivascular cuffs where it may contribute to leucocyte migration into the CNS parenchyma. Whether versican V1 is similarly elevated in other routes of passage of immune cells into the CNS, such as the pial membrane and choroid plexus, will be evaluated in the future. We do not know if leucocyte transmigration in the CNS parenchyma will always be correspondent with CSPG elevation, as there are likely other potential mediators and inhibitors of leucocyte mobility within the CNS. Nonetheless, our data do indicate that regulating CSPG production is a potential therapeutic strategy in multiple sclerosis to ameliorate leucocyte transmigration and their pro-inflammatory activity, and disease severity. In support, a previous report from our laboratory found that an inhibitor of CSPG synthesis improved outcomes in EAE (Keough *et al.*, 2016).

In conclusion, our findings provide novel insights into the roles and mechanisms of CSPGs, and identify them as a novel mediator of leucocyte transmigration and a therapeutic target in multiple sclerosis to alleviate neuroinflammation, neuropathology, and clinical severity.

Acknowledgements

We are grateful to Dr. Yan Fan for her technical support with immunohistochemical staining, Janet Wang for cell culture support, and Ms. Claudia Silva for technical support. We thank Dr. Lydia Sorokin for providing antibody to pan-laminin. We thank Dr. Richard Reynolds (UK Multiple Sclerosis Tissue Bank at Imperial College, London) for providing the post-mortem multiple sclerosis samples used in this study. Imaris rendering was supported by the Live Cell Imaging Facility, funded by the Snyder Institute at the University of Calgary, and by the Advanced Microscopy Platform of the Core Facility of the Hotchkiss Brain Institute.

Funding

This work was supported by operating grants from the Canadian Institutes of Health Research (CIHR) and the Alberta Innovates Health Solutions CRIO Team program. E.S. acknowledges studentship support from the CIHR

Vanier program and Alberta Innovates Health Solutions. V.W.Y. has salary support from the Canada Research Chair (Tier 1) program.

Supplementary material

Supplementary material is available at *Brain* online.

References

Agrawal S, Anderson P, Durbeej M, van Rooijen N, Ivars F, Opdenakker G, et al. Dystroglycan is selectively cleaved at the parenchymal basement membrane at sites of leukocyte extravasation in experimental autoimmune encephalomyelitis. J Exp Med 2006; 203: 1007–19.

Agrawal SM, Williamson J, Sharma R, Kebir H, Patel K, Prat A, et al. Extracellular matrix metalloproteinase inducer shows active perivascular cuffs in multiple sclerosis. Brain 2013; 136 (Pt 6): 1760–77.

Archambault AS, Sim J, Gimenez MA, Russell JH. Defining antigen-dependent stages of T cell migration from the blood to the central nervous system parenchyma. Eur J Immunol 2005; 35: 1076–85.

Bignami A, Hosley M, Dahl D. Hyaluronic acid and hyaluronic acid-binding proteins in brain extracellular matrix. Anat Embryol 1993; 188: 419–33.

Brocke S, Piercy C, Steinman L, Weissman IL, Veromaa T. Antibodies to CD44 and integrin alpha4, but not L-selectin, prevent central nervous system inflammation and experimental encephalomyelitis by blocking secondary leukocyte recruitment. Proc Natl Acad Sci USA 1999; 96: 6896–901.

Carulli D, Rhodes KE, Brown DJ, Bonnert TP, Pollack SJ, Oliver K, et al. Composition of perineuronal nets in the adult rat cerebellum and the cellular origin of their components. J Comp Neurol 2006; 494: 559–77.

Davies SJ, Fitch MT, Memberg SP, Hall AK, Raisman G, Silver J. Regeneration of adult axons in white matter tracts of the central nervous system. Nature 1996; 390: 680–3.

Dours-Zimmermann MT, Maurer K, Rauch U, Stoffel W, Fässler R, Zimmermann DR. Versican V2 assembles the extracellular matrix surrounding the nodes of ranvier in the CNS. J Neurosci 2009; 29: 7731–42.

Dutt S, Kléber M, Matasci M, Sommer L, Zimmermann DR. Versican V0 and V1 guide migratory neural crest cells. J Biol Chem 2006; 281: 12123–31.

Engelhardt B. Molecular mechanisms involved in T cell migration across the blood-brain barrier. J Neural Transm 2006; 113: 477–85.

Engelhardt B, Ransohoff RM. The ins and outs of T-lymphocyte trafficking to the CNS: anatomical sites and molecular mechanisms. Trends Immunol 2005; 26: 485–95.

Frohman EM, Racke MK, Raine CS. Multiple sclerosis–the plaque and its pathogenesis. N Engl J Med 2006; 354: 942–55.

Galtrey CM, Fawcett JW. The role of chondroitin sulfate proteoglycans in regeneration and plasticity in the central nervous system. Brain Res Rev 2007; 54: 1–18.

Galtrey CM, Kwok JC, Carulli D, Rhodes KE, Fawcett JW. Distribution and synthesis of extracellular matrix proteoglycans, hyaluronan, link proteins and tenascin-R in the rat spinal cord. Eur J Neurosci 2008; 27: 1373–90.

Gerwien H, Hermann S, Zhang X, Korpos E, Song J, Kopka K, et al. Imaging matrix metalloproteinase activity in multiple sclerosis as a specific marker of leukocyte penetration of the blood-brain barrier. Sci Transl Med 2016; 8: 364ra152.

Giuliani F, Metz LM, Wilson T, Fan Y, Bar-Or A, Yong VW. Additive effect of the combination of glatiramer acetate and minocycline in a model of MS. J Neuroimmunol 2005; 158: 213–21.

Goncalves DaSilva A, Yong VW. Matrix metalloproteinase-12 deficiency worsens relapsing-remitting experimental autoimmune encephalomyelitis in association with cytokine and chemokine dysregulation. Am J Pathol 2009; 174: 898–909.

Haylock-Jacobs S, Keough MB, Lau L, Yong VW. Chondroitin sulphate proteoglycans: extracellular matrix proteins that regulate immunity of the central nervous system. Autoimmun Rev 2011; 10: 766–72.

Jones TB, Hart RP, Popovich PG. Molecular control of physiological and pathological T-cell recruitment after mouse spinal cord injury. J Neurosci 2005; 25: 6576–83.

Kang I, Harten IA, Chang MY, Braun KR, Sheih A, Nivison MP, et al. Versican deficiency significantly reduces lung inflammatory response induced by polyinosine-polycytidylic acid stimulation. J Biol Chem 2017; 292: 51–63.

Kawashima H, Atarashi K, Hirose M, Hirose J, Yamada S, Sugahara K, et al. Oversulfated chondroitin/dermatan sulfates containing GlcAbeta1/IdoAalpha1-3GalNAc(4,6-O-disulfate) interact with L- and P-selectin and chemokines. J Biol Chem 2002; 277: 12921–30.

Kawashima H, Hirose M, Hirose J, Nagakubo D, Plaas AH, Miyasaka M. Binding of a large chondroitin sulfate/dermatan sulfate proteoglycan, versican, to L-selectin, P-selectin, and CD44. J Biol Chem 2000; 275: 35448–56.

Keough MB, Rogers JA, Zhang P, Jensen SK, Stephenson EL, Chen T, et al. An inhibitor of chondroitin sulfate proteoglycan synthesis promotes central nervous system remyelination. Nat Commun 2016; 7: 11312.

Kerfoot SM, Kubes P. Overlapping roles of P-selectin and alpha 4 integrin to recruit leukocytes to the central nervous system in experimental autoimmune encephalomyelitis. J Immunol 2002; 169: 1000–6.

Kim S, Takahashi H, Lin WW, Descargues P, Grivennikov S, Kim Y, et al. Carcinoma-produced factors activate myeloid cells through TLR2 to stimulate metastasis. Nature 2009; 457: 102–6.

Kolset SO, Kjellén L, Seljelid R, Lindahl U. Changes in glycosaminoglycan biosynthesis during differentiation *in vitro* of human monocytes. Biochem J 1983; 210: 661–7.

Kuipers HF, Rieck M, Gurevich I, Nagy N, Butte MJ, Negrin RS, et al. Hyaluronan synthesis is necessary for autoreactive T-cell trafficking, activation, and Th1 polarization. Proc Natl Acad Sci USA 2016; 113: 1339–44.

Laflamme N, Soucy G, Rivest S. Circulating cell wall components derived from gram-negative, not gram-positive, bacteria cause a profound induction of the gene-encoding Toll-like receptor 2 in the CNS. J Neurochem 2001; 79: 648–57.

Landolt RM, Vaughan L, Winterhalter KH, Zimmermann DR. Versican is selectively expressed in embryonic tissues that act as barriers to neural crest cell migration and axon outgrowth. Development 1995; 121: 2303–12.

Lau LW, Keough MB, Haylock-Jacobs S, Cua R, Döring A, Sloka S, et al. Chondroitin sulfate proteoglycans in demyelinated lesions impair remyelination. Ann Neurol 2012; 72: 419–32.

Levitt D, Ho PL. Induction of chondroitin sulfate proteoglycan synthesis and secretion in lymphocytes and monocytes. J Cell Biol 1983; 97: 351–8.

Lindahl P, Johansson BR, Levéen P, Betsholtz C. Pericyte loss and microaneurysm formation in PDGF-B-deficient mice. Science 1997; 277: 242–5.

Martinez FO, Gordon S, Locati M, Mantovani A. Transcriptional profiling of the human monocyte-to-macrophage differentiation and polarization: new molecules and patterns of gene expression. J Immunol 2006; 177: 7303–11.

Matthews RT, Kelly GM, Zerillo CA, Gray G, Tiemeyer M, Hockfield S. Aggrecan glycoforms contribute to the molecular heterogeneity of perineuronal nets. J Neurosci 2002; 22: 7536–47.

McKeon RJ, Schreiber RC, Rudge JS, Silver J. Reduction of neurite outgrowth in a model of glial scarring following CNS injury is correlated with the expression of inhibitory molecules on reactive astrocytes. J Neurosci 1991; 11: 3398–411.

Morawski M, Brückner G, Arendt T. Aggrecan: beyond cartilage and into the brain. Int J Biochem Cell Biol 2012; 44: 690–3.

Noseworthy JH, Lucchinetti C, Rodriguez M, Weinshenker BG. Multiple sclerosis. N Engl J Med 2000; 343: 938–52.

Owens T, Bechmann I, Engelhardt B. Perivascular spaces and the two steps to neuroinflammation. J Neuropathol Exp Neurol 2008; 67: 1113–21.

Parish CR. The role of heparan sulphate in inflammation. Nat Rev Immunol 2006; 6: 633–43.

Radeke HH, Ludwig RJ, Boehncke WH. Experimental approaches to lymphocyte migration in dermatology in vitro and *in vivo*. Exp Dermatol 2005; 14: 641–66.

Ransohoff RM, Engelhardt B. The anatomical and cellular basis of immune surveillance in the central nervous system. Nat Rev Immunol 2012; 12: 623–35.

Sobel RA, Ahmed AS. White matter extracellular matrix chondroitin sulfate/dermatan sulfate proteoglycans in multiple sclerosis. J Neuropathol Exp Neurol 2001; 60: 1198–207.

Sorokin L. The impact of the extracellular matrix on inflammation. Nat Rev Immunol 2010; 10: 712–23.

Tang X, Davies JE, Davies SJ. Changes in distribution, cell associations, and protein expression levels of NG2, neurocan, phosphacan, brevican, versican V2, and tenascin-C during acute to chronic maturation of spinal cord scar tissue. J Neurosci Res 2003; 71: 427–44.

Toeda K, Nakamura K, Hirohata S, Hatipoglu OF, Demircan K, Yamawaki H, et al. Versican is induced in infiltrating monocytes in myocardial infarction. Mol Cell Biochem 2005; 280: 47–56.

Toft-Hansen H, Buist R, Sun XJ, Schellenberg A, Peeling J, Owens T. Metalloproteinases control brain inflammation induced by pertussis toxin in mice overexpressing the chemokine CCL2 in the central nervous system. J Immunol 2006; 177: 7242–9.

Tran EH, Hoekstra K, van Rooijen N, Dijkstra CD, Owens T. Immune invasion of the central nervous system parenchyma and experimental allergic encephalomyelitis, but not leukocyte extravasation from blood, are prevented in macrophage-depleted mice. J Immunol 1998; 161: 3767–75.

Trapp BD, Nave KA. Multiple sclerosis: an immune or neurodegenerative disorder? Annu Rev Neurosci 2008; 31: 247–69.

Uhlin-Hansen L, Eskeland T, Kolset SO. Modulation of the expression of chondroitin sulfate proteoglycan in stimulated human monocytes. J Biol Chem 1989; 264: 14916–22.

Warren JR. Polymyxin B suppresses the endotoxin inhibition of concanavalin a-mediated erythrocyte agglutination. Infect Immun 1982; 35: 594–9.

Weaver A, Goncalves da Silva A, Nuttall RK, Edwards DR, Shapiro SD, Rivest S, et al. An elevated matrix metalloproteinase (MMP) in an animal model of multiple sclerosis is protective by affecting Th1/Th2 polarization. FASEB J 2005; 19: 1668–70.

Wu C, Ivars F, Anderson P, Hallmann R, Vestweber D, Nilsson P, et al. Endothelial basement membrane laminin alpha5 selectively inhibits T lymphocyte extravasation into the brain. Nat Med 2009; 15: 519–27.

Yong VW. Metalloproteinases: mediators of pathology and regeneration in the CNS. Nat Rev Neurosci 2005; 6: 931–44.

Zheng PS, Vais D, Lapierre D, Liang YY, Lee V, Yang BL, et al. PG-M/versican binds to P-selectin glycoprotein ligand-1 and mediates leukocyte aggregation. J Cell Sci 2004; 117 (Pt 24): 5887–95.